

Accelerating Plug-and-Play Image Reconstruction via Multi-Stage Sketched Gradients

Junqi Tang

Department of Applied Mathematics and Theoretical Physics (DAMTP),
University of Cambridge

JT814@CAM.AC.UK

Abstract

In this work we propose a new paradigm for designing fast plug-and-play (PnP) algorithms using dimensionality reduction techniques. Unlike existing approaches which utilize stochastic gradient iterations for acceleration, we propose novel multi-stage sketched gradient iterations which first perform downsampling dimensionality reduction in the image space, and then efficiently approximate the true gradient using the sketched gradient in the low-dimensional space. This sketched gradient scheme can also be naturally combined with PnP-SGD methods for further improvement on computational complexity. As a generic acceleration scheme, it can be applied to accelerate any existing PnP/RED algorithm. Our numerical experiments on X-ray fan-beam CT demonstrate the remarkable effectiveness of our scheme, that a computational free-lunch can be obtained using this dimensionality reduction in the image space.

1. Introduction

Iterative model-based reconstruction algorithms have been the de-facto techniques for solving imaging inverse problems such as image deblurring/inpainting/superresolution and tomographic image reconstruction (for example X-ray CT, MRI and PET, etc). Due to their strengths in delivering data-consistent and robust reconstruction, these iterative solvers, especially when combined with advanced image priors (Dabov et al., 2007; Zhang et al., 2017; Tachella et al., 2021) in a “plug-and-play” (PnP) manner (Egiazarian et al., 2007; Venkatakrishnan et al., 2013; Romano et al., 2017; Reehorst and Schniter, 2018), can still thrive in current era where deep neural networks (Jin et al., 2017) have been successfully adopted in all these problems.

In this work, we propose a new paradigm of designing fast PnP algorithms utilizing the principle of dimension reduction in solving high-dimensional/resolution imaging inverse problems. Such imaging systems can be generally expressed as:

$$b = Ax^\dagger + w, \quad (1)$$

where $x^\dagger \in \mathbb{R}^d$, $A \in \mathbb{R}^{n \times d}$, $b \in \mathbb{R}^n$ and $w \in \mathbb{R}^n$ denote the ground truth image, the forward operator which models the measurement physics, the measurement data, and the measurement noise in the data (the noise can be data-dependent), respectively.

Traditionally, to obtain an estimate of the ground truth x^\dagger , we typically solve an optimization problem of the form:

$$x^* \in \arg \min_{x \in \mathbb{R}^d} f(b, Ax) + g(x), \quad (2)$$

where data fidelity term $f(b, Ax)$ is a convex function in x , and the most typical and widely used choice of the data fidelity would be the least-squares loss $\|b - Ax\|_2^2$. The $g(x)$ here is a regularization function which is usually convex to ensure provable convergence and robustness of the estimation, such as the TV

regularization applied on image domain and ℓ_1 regularization in wavelet/shearlet domain. This optimization problem can be efficiently solved by proximal splitting methods (Combettes and Pesquet, 2011) for example FISTA (Beck and Teboulle, 2009) and ADMM (Boyd et al., 2011).

While these classical convex regularization approaches provide theoretically tractable solutions for inverse problems, they have been significantly outperformed by the PnP priors, constructed by advanced image denoisers or deep neural networks. The very first PnP algorithm (probably not very well-known) is actually proposed by Egiazarian et al. (2007), which is a PnP stochastic approximation algorithm with BM3D as the denoiser. The PnP-ADMM of Venkatakrishnan et al. (2013) and PnP-FISTA of Kamilov et al. (2017) extend the classical methods ADMM and FISTA, replacing the proximal operator with the denoiser and have been widely applied in solving inverse problems since then. Then a very similar approach named regularization-by-denoising (RED) has been proposed by Romano et al. (2017); Reehorst and Schniter (2018), which explicitly construct the regularization term using the denoiser and provide improved convenience in parameter tuning. Since a strong link between PnP and RED is established in Cohen et al. (2021) under the RED-PRO unifying framework, in this work we refer both plug-and-play and regularization-by-denoising as ‘‘PnP’’ for simplicity.

For large-scale problems, the PnP-ADMM and PnP-FISTA may require long computational time to obtain a good estimate. The PnP-SGD (Sun et al., 2019) and stochastic PnP-ADMM methods (Tang and Davies, 2020; Sun et al., 2020) can provide significant acceleration compared to the deterministic PnP-ADMM/PnP-FISTA methods. In this work we propose a generic acceleration of PnP gradient methods using dimensionality-reduction/sketching in the image-space.

2. Multi-Stage Sketched Plug-and-Play

In this section we present our multi-stage sketched gradient framework PnP-MS2G. The sketching techniques have been widely applied in large-scale optimization especially the least-squares problems (Pilanci and Wainwright, 2017, 2016, 2015; Tang et al., 2017a,b). However, the author has found that such data-domain sketching methods are not efficient in imaging inverse problems, since very often the forward operator is relatively sparse, and even the most efficient sparse Johnson-Lindenstrauss transform (Woodruff et al., 2014) cannot provide significant computational gain here since the sketched operator typically has similar sparsity as the full operator. If we use subsampling sketch which is the only practical data-domain sketch, the performance is similar or worse than SGD methods in imaging inverse problems.

Instead of using data-domain sketches, we propose to perform sketching in image-domain which appears to be much more effective and can be applied to generically accelerate PnP gradient methods such as PnP-FISTA and PnP-SGD.

2.1 Algorithmic Framework

Suppose the original objective reads:

$$x^* \in \arg \min_{x \in \mathbb{R}^d} f(b, Ax) + g(x), \quad (3)$$

where $g(x)$ can be some implicit non-convex regularization constructed by the denoiser (we write this for the ease of presentation), then our sketched objective can be generally expressed as:

$$x^* \in \arg \min_{x \in \mathbb{R}^d} f(b, A_s \mathcal{S}(x)) + g(x), \quad (4)$$

Algorithm 1 — Plug-and-Play with Multi-Stage Sketched Gradients (PnP-MS2G)

Initialization: $x_0 = y_0 \in \mathbb{R}^d$, number of stages K , sketch-size $[m_1, \dots, m_K]$, sketched forward operator $[A_{s_1}, \dots, A_{s_K}]$, sketching operators $[\mathcal{S}_1, \dots, \mathcal{S}_K]$, up-sampling operators $[\mathcal{U}_1, \dots, \mathcal{U}_K]$, number of inner-loops for each stage $[N_1, \dots, N_K]$, step-size sequence $[\eta_1, \dots, \eta_{\sum_{k=1}^K N_k}]$, momentum sequence $[a_1, \dots, a_{\sum_{k=1}^K N_k}]$, $\alpha \in (0, 1]$, iteration counter $i = 0$

for $k = 1$ **to** K **do**

for $j = 1$ **to** N_k **do**

$i \leftarrow i + 1$

Compute the sketch:

$v = \mathcal{S}_k(y_i)$

Compute gradient estimate G :

Option 1: $G := \nabla f_v(b, A_{s_k} v)$; or a stochastic gradient estimation of it:

Option 2: $G := \nabla f_v(M_i b, M_i A_{s_k} v)$ where M_i is a randomly sampled minibatch of $I_{n \times n}$.

$z_{i+1} = y_i - \eta_i \mathcal{U}_k G$,

$x_{i+1} = (1 - \alpha) z_{i+1} + \alpha \mathcal{D}(z_{i+1})$,

$y_{i+1} = x_{i+1} + a_i (x_{i+1} - x_i)$

end for

end for

Output x_{i+1}

where $\mathcal{S}(\cdot) : \mathbb{R}^d \rightarrow \mathbb{R}^m$ ($m < d$) being the sketching/downsampling operator, while $A_s \in \mathbb{R}^{n \times m}$ is the forward operator discretized on the reduced image space. We found that such a scheme provides a remarkably efficient approximation of the solution. We present our PnP-MS2G framework in Algorithm 1, where we denote \mathcal{D} as the denoiser, \mathcal{S} as the sketching operator, and \mathcal{U} as the upsampling operator.

To explain the motivation and derivation of Algorithm 1, we start by illustrating here a concrete example where the data-fidelity is the least-squares. Noting that the PnP proximal gradient descent iteration can be written as:

$$x_{k+1} = \mathcal{D}[x_k - \eta \cdot (A^T A x_k - A^T b)], \quad (5)$$

where $\mathcal{D}(\cdot)$ denotes the denoiser, which can be a denoising algorithm such as NLM/BM3D/TNRD, or a classical proximal operator of some convex regularization (such as TV-prox), or a pretrained denoising deep network such as (DnCNN). Then our sketched gradient can be written as:

$$x_{k+1} = \mathcal{D}[x_k - \eta \cdot \mathcal{U}(A_s^T A_s \mathcal{S}(x_k) - A_s^T b)], \quad (6)$$

where $\mathcal{U}(\cdot)$ denotes the upsampling operator. Numerically we found that off-the-shelf up/down-sampling algorithms such as the bi-cubic interpolation suffice to provide us good estimates of the true gradients. Using this scheme, an efficient approximation of the true gradient can be obtained since A_s only takes a fraction of the computation of A , and usually \mathcal{U} and \mathcal{S} can be very efficiently computed.

To further reduce the computational complexity, we can also utilize stochastic gradient estimate:

$$x_{k+1} = \mathcal{D}[y_k - \eta_k \cdot \mathcal{U}((M_k A_s)^T M_k A_s \mathcal{S}(y_k) - (M_k A_s)^T M_k b)] \quad (7)$$

where M_k is uniformly sampled minibatch of $I_{n \times n}$ here for computing the stochastic gradient. Here we use a vanilla minibatch stochastic gradient estimator. We can also choose here those advanced stochastic variance-reduced gradient estimator (Roux et al., 2012; Johnson and Zhang, 2013; Defazio et al., 2014;

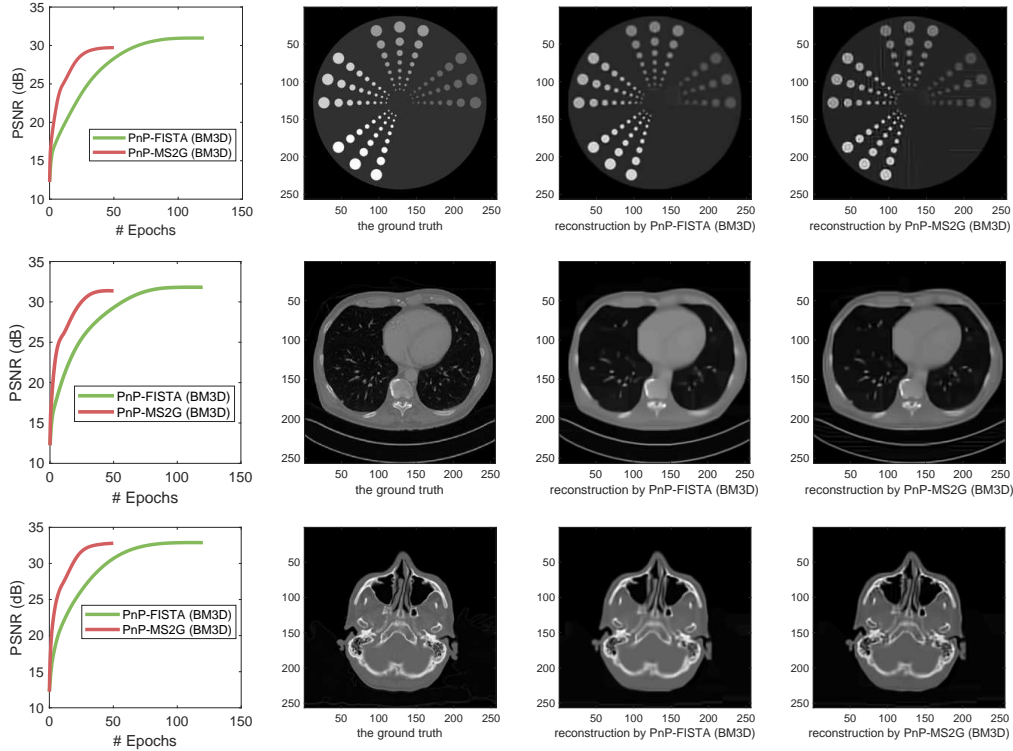


Figure 1: Numerical results for **Sparse-View** CT, with $I_0 = 1 \times 10^{5.5}$, $A \in \mathbb{R}^{20520 \times 65536}$, 90 view equally space from $[0, 360)$ degrees

Driggs et al., 2021) for potentially even faster convergence. Note that the stochastic gradient iterations do not necessary provide improved performance in all inverse problems – there are cases of inverse problems for which the stochastic methods do not provide faster convergence compared to deterministic methods (Tang et al., 2020). For compressed sensing MRI where we use subsampled FFT as forward operator, and even in CT/PET reconstruction if we use Non-uniform FFT (Fessler and Sutton, 2003; Tang, 2016) for fast approximation of the Radon transform, the stochastic gradient is not applicable since it will break the fast computational structure of FFT/NUFFT.

In Algorithm 1 we present our PnP-MS2G framework, where we typically start by an aggressive sketch $\{A_{s_1}, \mathcal{S}_1\}$ with $m_1 \ll d$ for very fast initial convergence, and then for later stages we switch to medium size sketches $\{A_{s_k}, \mathcal{S}_k\}$ with $m_k < d$ which are increasingly more conservative, to reach a similar reconstruction accuracy as the unsketched counterpart. Our algorithmic framework admit both deterministic gradient (Option 1) and stochastic gradient (Option 2), with momentum acceleration for which we recommend FISTA-type momentum (Beck and Teboulle, 2009; Chambolle and Dossal, 2015). For the denoising step we integrate the unifying RED-PRO (Cohen et al., 2021) framework here which includes both PnP (if we choose $\alpha = 1$) and RED as special cases.

We also wish to point out that in our sketching framework both the denoiser \mathcal{D} , the upsampling function \mathcal{U} and sketching function \mathcal{S} can be parameterized as deep (convolutional) neural-networks and trained either in a recursive or end-to-end manner, resulting in a new efficient deep-unrolling scheme (Adler and Öktem, 2018; Tang et al., 2021).

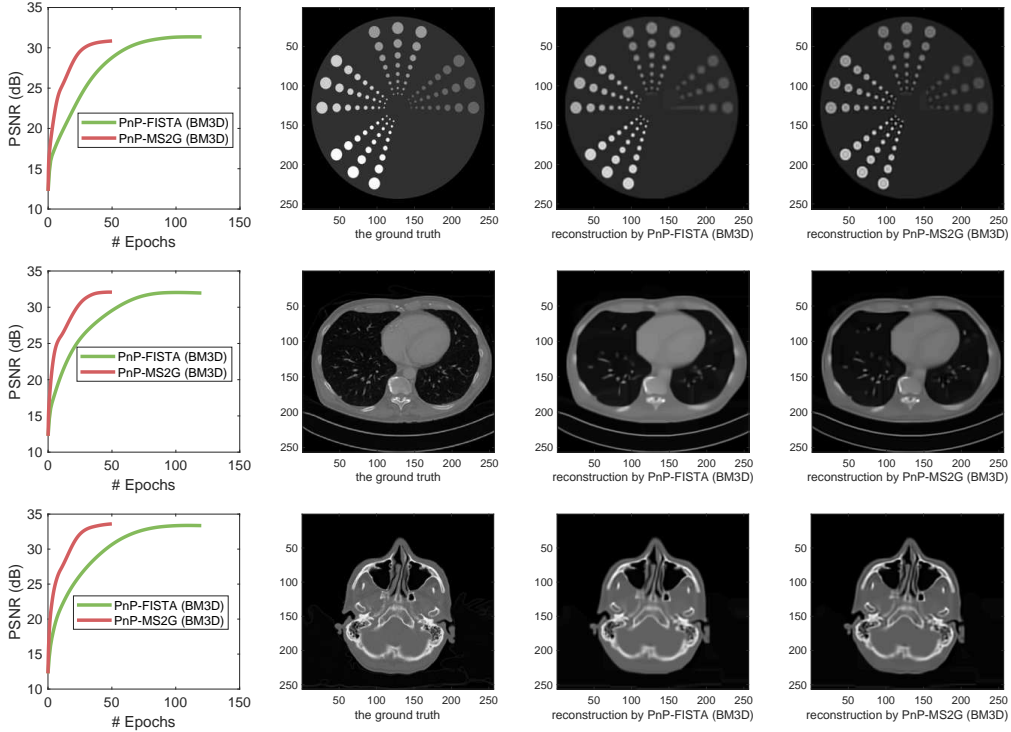


Figure 2: Numerical results for **Low-Dose** CT, with $I_0 = 1 \times 10^{3.5}$, $A \in \mathbb{R}^{82080 \times 65536}$, 360 view equally space from $[0, 360)$ degrees

In the multi-sketch framework presented here we gradually increase the sketch size m throughout stages. A seemingly plausible alternative could be modifying the iterative-Hessian-sketch framework proposed by [Pilanci and Wainwright \(2016\)](#) to sketch on the image domain. However in our initial experiments we found such a scheme is not as efficient as our PnP-MS2G and hence we do not report this alternative scheme here.

3. Numerical Experiments

In this section we present some numerical results for the proof-of-concept. We consider 3 fan-beam X-ray CT examples, sparse-view CT, low-dose CT, and limited angle CT. We simulate the noisy measurements (with Poisson noise):

$$b \sim \text{Poisson}(I_0 e^{-Ax^\dagger}), \quad (8)$$

and take the logarithmic of the data. All the experiments here are implemented and executed using MATLAB R2018b.

In all the experiments we use the BM3D ([Dabov et al., 2007](#)) as the denoiser for the PnP methods. We test the Option 1 (deterministic gradient) of PnP-MS2G and compare it to PnP-FISTA ([Kamilov et al., 2017](#)). For the up-sampling operator \mathcal{U} and sketching operator \mathcal{S} , we use the MATLAB `imresize` function with `bicubic` interpolation. We use 3 testing images (both sized 256×256): a phantom image with disks of various sizes, a head image, and a chest image. We use a fixed step-size $\eta = O(\frac{1}{L})$ where L is the gradient Lipschitz constant of the data-fidelity function and the momentum parameter $a_i = \frac{i-1}{i+3}$ adopted

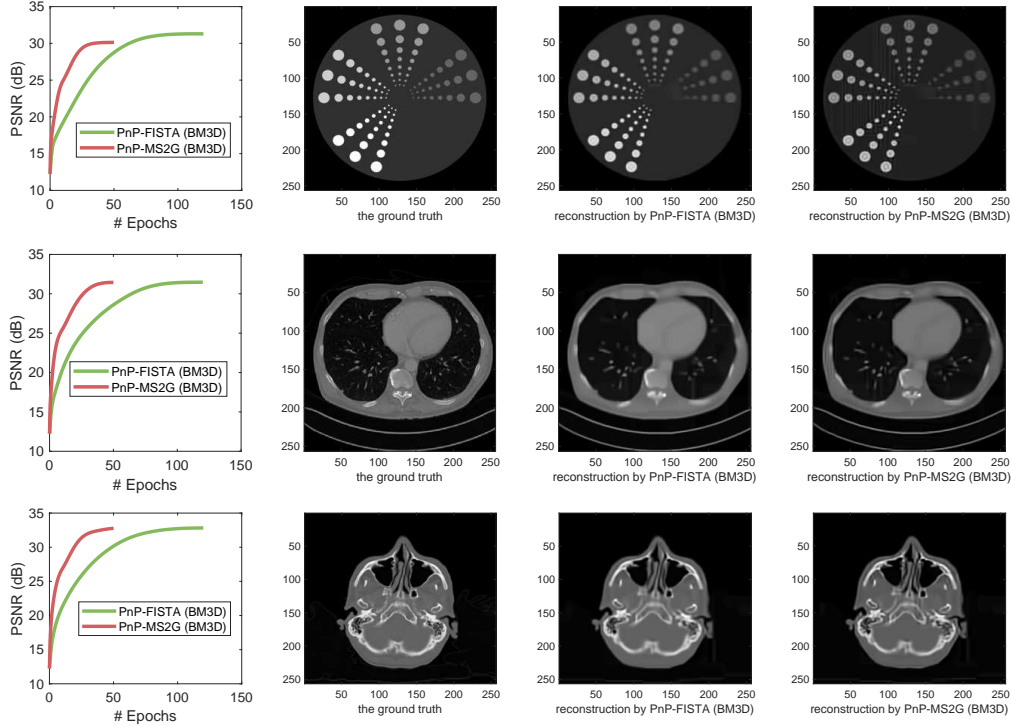


Figure 3: Numerical results for **Limited-Angle** CT, with $I_0 = 1 \times 10^{5.5}$, $A \in \mathbb{R}^{20520 \times 65536}$, 90 view equally space from $[0, 180)$ degrees

from the “convergent-FISTA” algorithm (Chambolle and Dossal, 2015) which has provable convergence on the variable. For simplicity we choose $\alpha = 1$ for PnP-MS2G. Meanwhile for PnP-MS2G we choose the number of stages as 2, where for the first stage we use 16-fold reduction on the dimension ($m_1 = \frac{d}{16}$), and for the second stage we use 4-fold reduction ($m_2 = \frac{d}{4}$)

We present our sparse view CT results in Figure 1, low-dose CT results in Figure 2, and limited angle CT results in Figure 3. We can observe that for all these examples our PnP-MS2G with deterministic gradient (Option 1) achieves almost the same reconstruction accuracy in PSNR compared to its full counterpart PnP-FISTA, while only requires a fraction of the computation of it. These results demonstrates that our proposed scheme for reducing the computational cost of PnP gradient methods is remarkably effective.

4. Conclusion

In this work we proposed a generic acceleration framework for accelerating gradient-based PnP/RED methods, exploiting the low-dimensional structure of the images which allowed us to efficiently approximate the gradient in the high-dimensional image space via dimensionality reduction schemes. In principle, our proposed multi-stage sketching framework can be readily applied to accelerate any existing deterministic/stochastic PnP/RED/Unrolling scheme. Our numerical experiments on sparse-view/low-dose/limited-angle CT demonstrate the effectiveness and huge potential of our framework.

This generic acceleration scheme can be easily applied to the cases where the non-uniform FFT (NUFFT) is used to provide fast computation of the forward operator (the NUFFT acceleration can be applied to both

MRI/CT/PET). In such cases the stochastic gradients cannot be efficiently applied since it will break the fast computation of FFT.

References

- Jonas Adler and Ozan Öktem. Learned primal-dual reconstruction. *IEEE transactions on medical imaging*, 37(6):1322–1332, 2018.
- A. Beck and M. Teboulle. Fast gradient-based algorithms for constrained total variation image denoising and deblurring problems. *IEEE Transactions on Image Processing*, 18(11):2419–2434, 2009.
- Stephen Boyd, Neal Parikh, Eric Chu, Borja Peleato, Jonathan Eckstein, et al. Distributed optimization and statistical learning via the alternating direction method of multipliers. *Foundations and Trends® in Machine learning*, 3(1):1–122, 2011.
- Antonin Chambolle and Ch Dossal. On the convergence of the iterates of the “fast iterative shrinkage/thresholding algorithm”. *Journal of Optimization theory and Applications*, 166(3):968–982, 2015.
- Regev Cohen, Michael Elad, and Peyman Milanfar. Regularization by denoising via fixed-point projection (red-pro). *SIAM Journal on Imaging Sciences*, 14(3):1374–1406, 2021.
- Patrick L Combettes and Jean-Christophe Pesquet. Proximal splitting methods in signal processing. In *Fixed-point algorithms for inverse problems in science and engineering*, pages 185–212. Springer, 2011.
- K Dabov, A Foi, V Katkovnik, and K Egiazarian. Image denoising by sparse 3-d transform-domain collaborative filtering. *IEEE transactions on image processing: a publication of the IEEE Signal Processing Society*, 16(8):2080–2095, 2007.
- A. Defazio, F. Bach, and S. Lacoste-Julien. Saga: A fast incremental gradient method with support for non-strongly convex composite objectives. In *Advances in Neural Information Processing Systems*, pages 1646–1654, 2014.
- Derek Driggs, Junqi Tang, Jingwei Liang, Mike Davies, and Carola-Bibiane Schonlieb. A stochastic proximal alternating minimization for nonsmooth and nonconvex optimization. *SIAM Journal on Imaging Sciences*, 14(4):1932–1970, 2021.
- Karen Egiazarian, Alessandro Foi, and Vladimir Katkovnik. Compressed sensing image reconstruction via recursive spatially adaptive filtering. In *2007 IEEE International Conference on Image Processing*, volume 1, pages I–549. IEEE, 2007.
- Jeffrey A Fessler and Bradley P Sutton. Nonuniform fast fourier transforms using min-max interpolation. *IEEE transactions on signal processing*, 51(2):560–574, 2003.
- Kyong Hwan Jin, Michael T McCann, Emmanuel Froustey, and Michael Unser. Deep convolutional neural network for inverse problems in imaging. *IEEE Transactions on Image Processing*, 26(9):4509–4522, 2017.
- Rie Johnson and Tong Zhang. Accelerating stochastic gradient descent using predictive variance reduction. In *Advances in neural information processing systems*, pages 315–323, 2013.

- Ulugbek S Kamilov, Hassan Mansour, and Brendt Wohlberg. A plug-and-play priors approach for solving nonlinear imaging inverse problems. *IEEE Signal Processing Letters*, 24(12):1872–1876, 2017.
- M. Pilanci and M. J. Wainwright. Randomized sketches of convex programs with sharp guarantees. *Information Theory, IEEE Transactions on*, 61(9):5096–5115, 2015.
- M. Pilanci and M. J. Wainwright. Iterative hessian sketch: Fast and accurate solution approximation for constrained least-squares. *Journal of Machine Learning Research*, 17(53):1–38, 2016.
- Mert Pilanci and Martin J Wainwright. Newton sketch: A near linear-time optimization algorithm with linear-quadratic convergence. *SIAM Journal on Optimization*, 27(1):205–245, 2017.
- Edward T Reehorst and Philip Schniter. Regularization by denoising: Clarifications and new interpretations. *IEEE Transactions on Computational Imaging*, 5(1):52–67, 2018.
- Yaniv Romano, Michael Elad, and Peyman Milanfar. The little engine that could: Regularization by denoising (red). *SIAM Journal on Imaging Sciences*, 10(4):1804–1844, 2017.
- Nicolas L. Roux, Mark Schmidt, and Francis R. Bach. A stochastic gradient method with an exponential convergence rate for finite training sets. In F. Pereira, C. J. C. Burges, L. Bottou, and K. Q. Weinberger, editors, *Advances in Neural Information Processing Systems 25*, pages 2663–2671. Curran Associates, Inc., 2012.
- Yu Sun, Brendt Wohlberg, and Ulugbek S Kamilov. An online plug-and-play algorithm for regularized image reconstruction. *IEEE Transactions on Computational Imaging*, 2019.
- Yu Sun, Zihui Wu, Brendt Wohlberg, and Ulugbek S Kamilov. Scalable plug-and-play admm with convergence guarantees. *arXiv preprint arXiv:2006.03224*, 2020.
- Julián Tachella, Junqi Tang, and Mike Davies. The neural tangent link between cnn denoisers and non-local filters. *IEEE/CVF Conference on Computer Vision and Pattern Recognition*, 2021.
- Junqi Tang. The non-uniform fast fourier transform in computed tomography. *arXiv preprint arXiv:1605.05231*, 2016.
- Junqi Tang and Mike Davies. A fast stochastic plug-and-play admm for imaging inverse problems. *arXiv preprint arXiv:2006.11630*, 2020.
- Junqi Tang, Mohammad Golbabaee, and Mike Davies. Exploiting the structure via sketched gradient algorithms. In *2017 IEEE Global Conference on Signal and Information Processing (GlobalSIP)*, pages 1305–1309. IEEE, 2017a.
- Junqi Tang, Mohammad Golbabaee, and Mike E. Davies. Gradient projection iterative sketch for large-scale constrained least-squares. In *Proceedings of the 34th International Conference on Machine Learning*, volume 70 of *Proceedings of Machine Learning Research*, pages 3377–3386. PMLR, 2017b.
- Junqi Tang, Karen Egiazarian, Mohammad Golbabaee, and Mike Davies. The practicality of stochastic optimization in imaging inverse problems. *IEEE Transactions on Computational Imaging*, 6:1471–1485, 2020.

Junqi Tang, Subhadip Mukherjee, and Carola-Bibiane Schonlieb. Stochastic primal-dual deep unrolling for imaging inverse problems. *arXiv preprint arXiv:2110.10093*, 2021.

Singanallur V Venkatakrisnan, Charles A Bouman, and Brendt Wohlberg. Plug-and-play priors for model based reconstruction. In *2013 IEEE Global Conference on Signal and Information Processing*, pages 945–948. IEEE, 2013.

David P Woodruff et al. Sketching as a tool for numerical linear algebra. *Foundations and Trends® in Theoretical Computer Science*, 10(1–2):1–157, 2014.

Kai Zhang, Wangmeng Zuo, Yunjin Chen, Deyu Meng, and Lei Zhang. Beyond a gaussian denoiser: Residual learning of deep cnn for image denoising. *IEEE Transactions on Image Processing*, 26(7):3142–3155, 2017.